

Foldamer-templated catalysis of macrocycle formation

Authors: Zebediah C. Girvin, Mary Katherine Andrews, Xinyu Liu, Samuel H. Gellman

Department of Chemistry, University of Wisconsin-Madison, 1101 University Avenue, Madison, Wisconsin 53706, United States

Abstract: Macrocycles, compounds containing a ring of 12 or more atoms, find use in human medicine, fragrances and biological ion sensing. The efficient preparation of macrocycles is a fundamental challenge in synthetic organic chemistry because the high entropic cost of large ring closure allows undesired intermolecular reactions to compete. Here we present a bio-inspired strategy for macrocycle formation via carbon-carbon bond formation. The process relies on a catalytic oligomer containing α - and β -amino acid residues to template the ring-closing process. The α/β -peptide foldamer adopts a helical conformation that displays a catalytic primary amine/secondary amine diad in a specific three-dimensional arrangement. This catalyst promotes aldol reactions that form rings containing 14-22 atoms. Utility is demonstrated in the synthesis of the natural product robustol.

One Sentence Summary: An enzyme-inspired foldamer catalyzes efficient formation of molecules containing 14- to 22-membered rings.

Macrocyclic compounds, containing a ring of 12 or more atoms, play important roles in biology and medicine (1-3). Engineered macrocycles have engendered new technologies (4) and new therapeutic strategies (5). Efficient synthesis of macrocycles is challenging as the entropic penalty associated with ring closure allows competition from intermolecular side-reactions, reducing yields of the desired products (6-10). Preorganization of linear precursors via multipoint coordination of a metal cation, an anion or a neutral partner can facilitate synthesis of specific macrocycle classes (Fig. 1), but this strategy depends on non-covalent interaction sites within the linear precursor (9-12). Intramolecular alkene metathesis can be very effective for formation of large rings (9, 13-15). This process features catalytic metal-based activation of terminal alkenes in a linear precursor, but additional coordination between internal functionality and the metal center is necessary (9, 13-16). Biosynthetic machinery overcomes the entropic cost of macrocycle formation by holding linear precursors in appropriate conformations, catalyzing the ring-closure reaction and inhibiting competing intermolecular processes (17, 18). We took inspiration from biological catalysts to develop a macrocyclization catalyst in which a well-folded oligomer activates both ends of a linear precursor and orients the termini for reaction, thereby serving as a template for ring closure via carbon-carbon bond formation.

Our approach uses a foldamer designed to facilitate macrocyclization via aldol condensation by proper orientation of two catalytic groups. We build on pioneering work by Miller et al., who employed related design principles to achieve site-specific catalytic functionalization of complex substrates (19). Our work complements the development of small molecules that serve as bifunctional catalysts, such as the recent mimicry of glycotransferase enzymes with cyclic bis-thioureas (20) and the recent stereoselective formation of nucleoside phosphoroamidates with bis-imidazoles (21). Neither of these cases, however, involved macrocycle formation.

Oligomer **1** (Fig. 2) contains both α - and β -amino acid residues and features an $\alpha\beta\beta$ backbone repeat pattern, which favors a helical conformation that has approximately three residues per turn (22, 23). Use of β residues with a five-membered ring constraint, such as the cyclopentane- and pyrrolidine-based residues in **1**, enhances helix stability (22). A related α/β -peptide containing two pyrrolidine-based residues catalyzes intermolecular crossed aldol condensations involving formaldehyde as the electrophile (24). Optimal catalysis required $i,i+3$ spacing of the pyrrolidine residues, which causes alignment of these two catalytic units upon helical folding. α/β -Peptide **1** is distinct from the earlier example in that one of the catalytic units is a primary amine, a difference that proved to be consequential.

The current study began with an unexpected observation. We asked whether α/β -peptide **1** would promote cyclization of C9 dialdehyde **A** to form cyclooctene-1-aldehyde (Fig. 2). The reaction conditions, based on precedents from Pihko et al. and our previous studies (24, 25), included propionic acid and triethylamine as additives and aqueous isopropanol as solvent. The cyclooctene derivative, however, was not observed when 10 mM **A** was allowed to react in the presence of 10 mol% **1**, although **A** appeared to be fully consumed within 24 hours. Instead, the foldamer catalyzed formation of a product mixture in which the principal components were cyclodimers. We isolated and identified the major cyclodimer by 2D NMR to be the 16-membered ring *E,E* diene **B**. LC-MS revealed initial formation of intermolecular aldol adduct **C**, but the amount of this intermediate remained low throughout the reaction, suggesting rapid cyclization. In contrast, a 1:1 mixture of pyrrolidine and n-butylamine (10 mol% each) catalyzed slow formation of the linear dimer **C**, with only trace levels of cyclodimer detected after 24 hours. We hypothesized that the foldamer acts by a bifunctional mechanism, serving as a template to overcome the entropic cost of large ring closure.

To gain further insight on the capabilities of foldamer **1**, we prepared symmetrical dialdehydes **D1-D4** (Fig. 3), each containing a central methoxyphenyl ring that allowed us to monitor starting material, products, and transient intermediates via UV absorbance. Initial studies focused on **D3**, which can form a 16-membered ring enal, matching the ring size of cyclodimer **B**. When we reacted **D3** with **1**, we observed nearly full conversion to macrocyclic *E*-enal **E3** (see supplementary material for full characterization). In contrast, the control reaction with pyrrolidine and n-butylamine produced only a trace amount of **E3** after 24 hours (Fig. S10).

α/β -Peptide **1** proved to be versatile in terms of product ring size (Fig. 3). We observed efficient conversion of **D4** to 18-membered ring *E*-enal **E4** and of **D2** to 14-membered ring *E*-enal **E2**. The foldamer-catalyzed reaction of **D1**, took longer to reach completion and led to a mixture of *E*-enal **E1** and cyclodimers. Precedents suggest that this outcome arises because of strain that develops upon 12-membered ring formation (7, 8). On the other hand, efficient and stereospecific synthesis of the 14-, 16- and 18-membered ring enals suggests that catalyst **1** is broadly competent for formation of larger rings.

Comparing formation of enal **E3** with α/β -peptide **1** and a set of related oligomers reveals that catalytic efficacy is very sensitive to specific features of foldamer structure (Fig. 4). As noted above, a control mixture of pyrrolidine and n-butylamine was much less effective than α/β -peptide **1** at promoting macrocycle formation. Similarly low reactivity was observed for a pair of mono-functional α/β -peptides (**2 + 3**) that provide the secondary and primary amine groups as β residue side chains in separate molecules. These results are consistent with a bifunctional mechanism involving activation of the two aldehyde groups within a substrate on a single catalyst molecule. A bifunctional mechanism is further supported by the observation that

macrocyclization to form **E3** displayed first-order dependence on α/β -peptide **1** (Fig. S13, S14). 2D NMR studies of **1**, conducted in either d₇-isopropanol or d₃-methanol, revealed numerous NOEs consistent with the expected helical conformation (Fig. S31, S34) and the alignment of the primary and secondary amine side chains, which is essential for bifunctional catalysis.

The spacing between reactive side chains along the foldamer backbone is crucial for catalytic efficacy, as shown by the low yields obtained with α/β -peptides **4-6**, which are sequence-isomers of **1**. When the β residues bearing the reactive amine groups were adjacent in primary sequence (*i,i+1* spacing; **4**), macrocyclization was barely detectable. The isomers with *i,i+2* and *i,i+4* spacing, **5** and **6**, were poor catalysts as well. Since the helical conformation favored by the $\alpha\beta\beta$ backbone has three residues per turn (22), differences among **1** and sequence-isomers **4-6** support the conclusion that optimal catalysis requires alignment of the primary and secondary amine groups along the helix axis. When the β residues that provide the reactive groups were properly spaced (*i,i+3*), but the linker between the primary amino group and the backbone was lengthened, as in **7**, catalytic activity suffered. Thus, even if the primary and secondary amines are aligned along the helix axis, increased flexibility of the segment between the two amino groups appears to be deleterious. α/β -Peptide **8** is the diastereomer of **1** that differs only in the configuration at the backbone carbon bearing the primary amine side chain, a change expected to diminish helix stability (26). We observed only a low yield of enal **E3** with **8**, consistent with high sensitivity of the reaction to the spatial positioning of the amino groups provided by the foldamer scaffold. Overall, this set of comparisons shows that catalytic activity depends on the ability of the α/β -peptide backbone to achieve a specific arrangement of the primary amine/secondary amine diad.

The chemical nature of the amine groups is critical for intramolecular aldol condensation (Fig. S35-S46). α/β -Peptide **9** presents a diad of primary amino groups with the optimal sequence spacing, but the yield of 16-membered ring enal **E3** was substantially lower for this catalyst relative to α/β -peptide **1**. α/β -Peptide **10** presents a secondary amine diad, and in this case the macrocyclic product was barely detectable. The variations in catalytic efficacy among **1**, **9** and **10** may arise because primary amines favor imine adducts with aldehydes (27), while secondary amines favor enamine adducts (28). Macrocycle formation presumably requires the generation of an electrophilic iminium and nucleophilic enamine on a single catalyst scaffold, a combination that is favored by the reactive diad of **1**. Previously, we found that α/β -peptide **10** was an excellent catalyst for intermolecular crossed aldol reactions (24). The distinct catalytic profiles of α/β -peptides **1** and **10** show that once a favorable foldamer scaffold is identified, reaction selectivity can be achieved by modifying the catalytic groups.

The modest macrocycle yield obtained with **11** shows that swapping the primary and secondary amine group positions within the α/β -peptide backbone causes erosion of catalytic efficacy. This observation highlights the ability to explore diverse spatial arrangements of reactive groups that is provided by a foldamer scaffold, which is inherently modular. Tripeptide **12** features *i,i+2* spacing but is too small to adopt a stable helical conformation. This tripeptide was slightly more effective than the longer α/β -peptide with *i,i+2* spacing (**5**), which raises the possibility that a stable folded conformation can cause a modest diminution of intrinsic amine reactivity, perhaps because of steric hindrance.

The efficient foldamer-catalyzed macrocyclization introduced here may be useful for the synthesis of large-ring natural products, analogues of these natural products, and novel macrocycles of potential therapeutic utility. We could produce the 18-membered ring core of

nostocycline A (Fig. 5) (29) from dialdehyde **F** with 10 mol% **1** (Fig. 5). Because the substrate is unsymmetrical, two macrocyclic *E*-enals are possible. Both were formed in 75% total yield, with a 2.8:1 ratio. The identity of the major isomer was established by a crystal structure of the tosylhydrazone derivative.

We further demonstrated the utility of foldamer-catalyzed macrocyclization by achieving total synthesis of the natural product robustol (30), which contains a 22-membered ring (Fig. 6). This compound is related to the turriane family of natural products, several of which have been prepared by application of macrocycle-closing alkene or alkyne metathesis (31). Our route to an appropriate dialdehyde substrate began with two nickel-catalyzed reductive cross coupling reactions, pioneered by Weix et al. (32), to prepare boronate ester **R1** and phenol **R3**. Copper-catalyzed Chan-Lam-Evans coupling of these two compounds generated diester **R4** (33, 34), and redox manipulations provided dialdehyde **R5**. The foldamer-catalyzed reaction efficiently generated the desired 22-membered ring skeleton as a mixture of isomers (**R6**). Heating with Wilkinson's catalyst induced decarbonylation (35), and the resulting alkene mixture was hydrogenated to produce **R7**. The methyl groups were removed by treatment with excess BBr₃ to yield a single product with a ¹H NMR spectrum matching that of natural robustol (30).

Our results suggest that a broad range of macrocycles will be accessible through intramolecular aldol condensations catalyzed by foldamer **1**, with limitations arising when ring closure causes significant internal strain (7,8). Because polar groups (amine, carboxylic acid, hydroxyl) are abundant in the reaction medium, aldol macrocyclizations catalyzed by α/β -peptide **1** will likely display considerable functional group tolerance. Macroyclic compounds are of interest for pharmaceutical development, as exemplified by the hepatitis C drug vaniprevir (36), and our method should enable synthesis of novel and diverse candidates to support discovery of new therapeutic agents. Our use of a foldamer scaffold to achieve optimal arrangement of the primary amine/secondary amine diad was inspired by the role of protein scaffolds in positioning catalytic groups within enzyme active sites (37). The prevalence of β -amino acid residues in our foldamer backbone allows us to employ residue-based strategies for conformational preorganization (23), an opportunity that is not available for catalyst designs based entirely on α -amino acid residues. Well-characterized foldamer scaffolds allow systematic variation of the arrangement of a reactive group set, such as the primary amine/secondary amine diad in **1**, which is useful for catalyst optimization (24). Small-molecule scaffolds for bifunctional catalysis (38-40) may be less amenable to exploration of alternative geometries for a given functional group diad relative to foldamer-based skeletons because small molecules lack the modularity of foldamers. We speculate that the $\alpha\beta\beta$ backbone of **1**, and related backbones containing preorganized β - and/or γ -amino acid residues, will provide scaffolds that can be harnessed to enable bifunctional or polyfunctional catalysis of other useful reactions.

References and Notes:

1. E. A. Villar, D. Beglov, S. Chennamdhavuni, J. A. Porco Jr., D. Kozakov, S. Vajda, A. Whitty, How proteins bind macrocycles. *Nature Chemical Biology* **10**, 723-732 (2014).

2. K. R. Campos, P. J. Coleman, J. C. Alvarez, S. D. Dreher, R. M. Garbaccio, N. K. Terrett, R. D. Tillyer, M. D. Truppo, E. R. Parmee, The importance of synthetic chemistry in the pharmaceutical industry. *Science* **363**, 6424 (2019).
3. D. J. Newman, G. M. Cragg, *Macrocycles in Drug Discovery* 1-499 (2014).
4. M. Iyoda, J. Yamakawa, M. J. Rahman, Conjugated macrocycles: Concepts and applications. *Angew. Chem. Int. Ed.* **50**, 10522-10553 (2011).
5. A. Rosenquist, B. Samuelsson, P-O Johansson, M. D. Cummings, O. Lenz, P. Raboisson, K. Simmen, S. Vendeville, H. de Kock, M. Nilsson, A. Horvath, R. Kalmeijer, G. de las Rosa, M. Beumont-Mauviel, Discovery and development of Simeprevir (TMC435), a HCV NS3/4A protease inhibitor. *J. Med. Chem.* **57**, 1673-1693 (2014).
6. T. Gulder, P. S. Baran, Strained cyclophane natural products: Macrocyclization at its limits. *Nat. Prod. Reports.* **29**, 899-934 (2012).
7. C. Galli, L. Mandolini, The role of ring strain on the ease of ring closure of bifunctional chain molecules. *Eur. J. Org. Chem.* 3117-3125 (2000).
8. M. A. Casadei, C. Galli, L. Mandolini, Ring-closure reactions. 22. Kinetics of cyclization of diethyl (.omega.-bromoalkyl)malonates in the range of 4- to 21-membered rings. Role of ring strain., *J. Am. Chem. Soc.*, **106**, 1051-1056 (1984).
9. A. Furstner, Recent advancements in ring closing olefin metathesis. *Topics in Catalysis* **4**, 285-299 (1997).

10. V. Marti-Centelles, M. D. Pandey, M. I. Burguete, S. V. Luis, Macrocyclization reactions: The importance of conformational, configurational, and template-induced preorganization. *Chem. Rev.* **115**, 8736-8834 (2015).
11. C. J. Pedersen, Cyclic polyethers and their complexes with metal salts. *J. Am. Chem. Soc.* **89**, 2495-2496 (1967).
12. S. J. Rowan, S. J. Cantrill, G. R. L. Cousins, J. K. M. Sanders, J. F. Stoddart, Dynamic covalent chemistry, *Angew. Chem. Int. Ed.*, **41**, 898-952 (2002).
13. H. E. Blackwell, J. D. Sadowsky, R. J. Howard, J. N. Sampson, J. A. Chao, W. E. Steinmetz, D. J. O'Leary, R. H. Grubbs, Ring-closing metathesis of olefinic peptides: design, synthesis, and structural characterization of macrocyclic helical peptides. *J. Org. Chem.* **66**, 5291-5302 (2001).
14. X. Shen, T. T. Nguyen, M. J. Koh, D. Xu, A. W. H. Speed, R. R. Schrock, A. H. Hoveyda, Kinetically E-selective macrocyclic ring-closing metathesis. *Nature*, **541**, 380-385 (2017).
15. A. Sytniczuk, M. Dabrowski, L. Banach, M. Urban, S. Czarnocka-Sniadala, M. Milewski, A. Kajetanowicz, K. Grela, At long last: Olefin metathesis macrocyclization at high concentration. *J. Am. Chem. Soc.* **140**, 8895-8901 (2018).
16. J. R. Ludwig, P. M. Zimmerman, J. B. Gianino, C. S. Schindler, Iron(III)-catalyzed carbonyl-olefin metathesis, *Nature*, **533** 374-379 (2016).
17. D. L. Akey, J. D. Kittendorf, J. W. Giraldes, R. A. Fecik, D. H. Sherman, J. L. Smith, Structural basis for macrolactonization by the pikromycin thioesterase. *Nature Chemical Biology* **2**, 537-542 (2006).

18. F. Kopp, M. A. Marahiel, Macrocyclization strategies in polyketide and nonribosomal biosynthesis. *Nat. Prod. Rep.* **24**, 735-749 (2007).
19. C. A. Lewis, S. J. Miller, Site-selective derivatization and remodeling of erythromycin A by using simple peptide-based chiral catalysts. *Angew. Chem. Int. Ed.* **45**, 5616-5619 (2006).
20. Y. Park, K. C. Harper, N. Kuhl, E. U. Kwan, R. Y. Liu, E. N. Jacobsen, Macroyclic bis-thioureas catalyze stereospecific glycosylation reactions. *Science* **355**, 162-166 (2017).
21. D. A. DiRocco, Y. Ji, E. C. Sherer, A. Klapars, M. Reibarkh, J. Dropinski, R. Mathew, P. Maligres, A. M. Hyde, J. Limanto, A. Brunskill, R. T. Ruck, L-C. Campeau, I. W. Davies, A multifunctional catalyst that stereoselectively assembles prodrugs. *Science* **356**, 426-430 (2017).
22. S. H. Choi, I. Guzei, L. Spencer, S. H. Gellman, Crystallographic characterization of helical secondary structures in 2:1 and 1:2 α/β -peptides. *J. Am. Chem. Soc.* **131**, 2917-2924 (2009).
23. J. L. Price, E. B. Hadley, J. D. Steingruber, S. H. Gellman, Detection and analysis of chimeric tertiary structure via backbone thioester exchange: packing of an α -helix against an α/β -helix, *Angew. Chem. Int. Ed.* **49**, 368-371 (2010).
24. Z. C. Girvin, S. H. Gellman, Exploration of diverse reactive diad geometries for bifunctional catalysis via foldamer backbone variation. *J. Am. Chem. Soc.* **140**, 12476-12483 (2018).

25. A. Erkkila, P. M. Pihko, Mild organocatalytic α -methylenation of aldehydes. *J. Org. Chem.* **71**, 2538-2541 (2006).

26. E. Krause, M. Bienert, P. Schmieder, H. Wenschuh, The helix-destabilizing propensity scale of D-amino acids: the influence of side chain steric effects, *J. Am. Chem. Soc.* **122**, 4865-4870 (2000).

27. A. Erkkila, I. Majander, P. Pihko, Iminium catalysis, *Chem. Rev.* **107**, 5416-5470 (2007).

28. S. Mukherjee, J. W. Yang, S. Hoffmann, B. List, Asymmetric enamine catalysis, *Chem. Rev.* **107**, 5471-5569 (2007).

29. A. Ploutno, S. Carmeli, Nostocycline A, a novel antimicrobial cyclophane from the cyanobacterium *Nostoc* sp. *J. Nat. Prod.* **63**, 1524-1526 (2000).

30. J. R. Cannon, P. W. Chow, M. W. fuller, B. H. Hamilton, B. W. Metcalf, A. J. Power, Phenolic constituents of Grevillea Robusta (Proteaceaf). The structure of robustol, a novel macrocyclic phenol, *Aust. J. Chem.*, **26** 2257-2275 (1973).

31. A. Furstner, F. Stelzer, A. Rumbo, H. Krause, Total synthesis of the turrianes and evaluation of their DNA-cleaving properties. *Chem. Eur. J.*, **8** 1856-1871 (2002).

32. D. A. Everson, B. A. Jones, D. J. Weix, Replacing conventional carbon nucleophiles with electrophiles: Nickel-catalyzed reductive alkylation of aryl bromides and chlorides. *J. Am. Chem. Soc.* **134**, 6146-6159 (2012).

33. D. A. Evans, J. L. Katz, T. R. West, Synthesis of diaryl ethers through the copper-promoted arylation of phenols with arylboronic acids. An expedient synthesis of thyroxine. *Tetrahedron Letters*, **39**, 2937-2940 (1998).

34. P. Y. S. Lam, C. G. Clark, S. Saubern, J. Adams, M. P. Winters, D. M. T. Chan, A. Combs, New aryl/heteroaryl C-N bond cross-coupling via arylboronic acid/cuprate acetate arylation, *Tetrahedron Letters*, **39**, 2941-2944 (1998).

35. K. Ohno, J. Tsuji, Organic synthesis by means of noble metal compounds. XXXV. Novel decarbonylation reactions of aldehydes and acyl halides using rhodium complexes. *J. Am. Chem. Soc.* **90**, 99-107 (1968).

36. J. A. McCauley, et. al., Discovery of MK-1220: A macrocyclic inhibitor of hepatitis C virus NS3/4A protease with improved preclinical plasma exposure. *J. Med. Chem.* **53**, 2443-2463 (2010).

37. S. J. Benkovic, S. Hammes-Schiffer, A perspective on enzyme catalysis. *Science* **301**, 1196-1202 (2003).

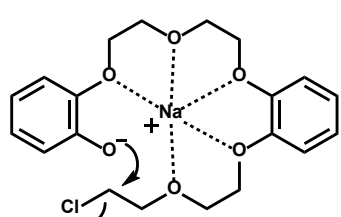
38. C. E. Song, *Cinchona Alkaloids in Synthesis and Catalysis, Ligands, Immobilization and Organocatalysis* Wiley-VCH: Weinheim, Germany (2008).

39. S-K. Tian, Y. Chen, J. Hang, L. Tang, P. McDaid, L. Deng, Asymmetric organic catalysis with modified cinchona alkaloids. *Acc. Chem. Res.* **37**, 621-631 (2004).

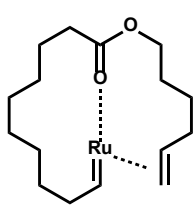
40. M. S. Taylor, E. N. Jacobsen, Asymmetric catalysis by chiral hydrogen-bond donors. *Angew. Chem. Int. Ed.* **45**, 1520-1543 (2006).

A

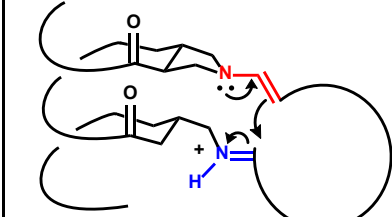
Macrocyclization Strategies



Guest-mediated cyclization



Ring-closing metathesis



This Work: Foldamer catalysis

B

Foldamer vs. Small Molecule Catalysis

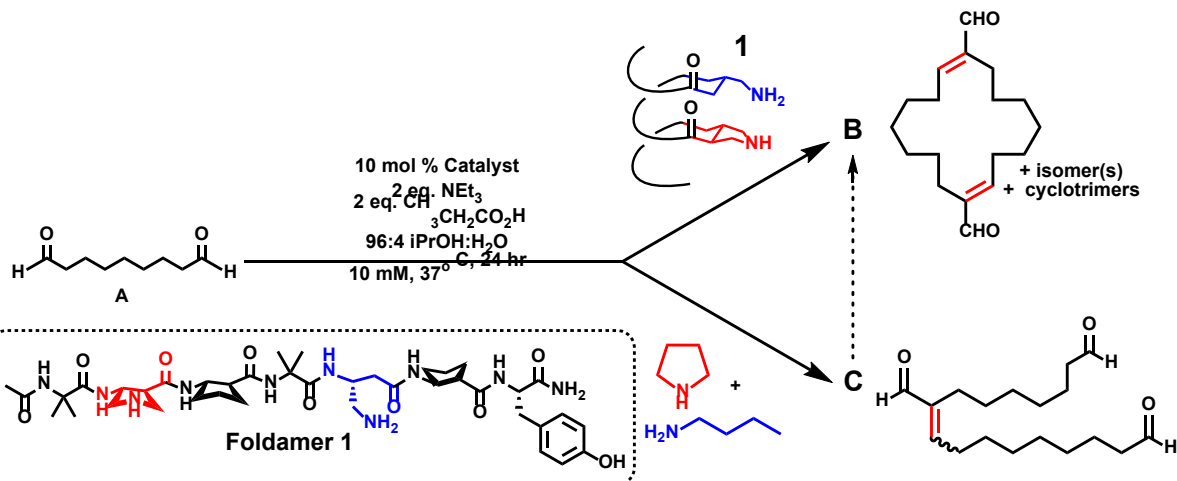
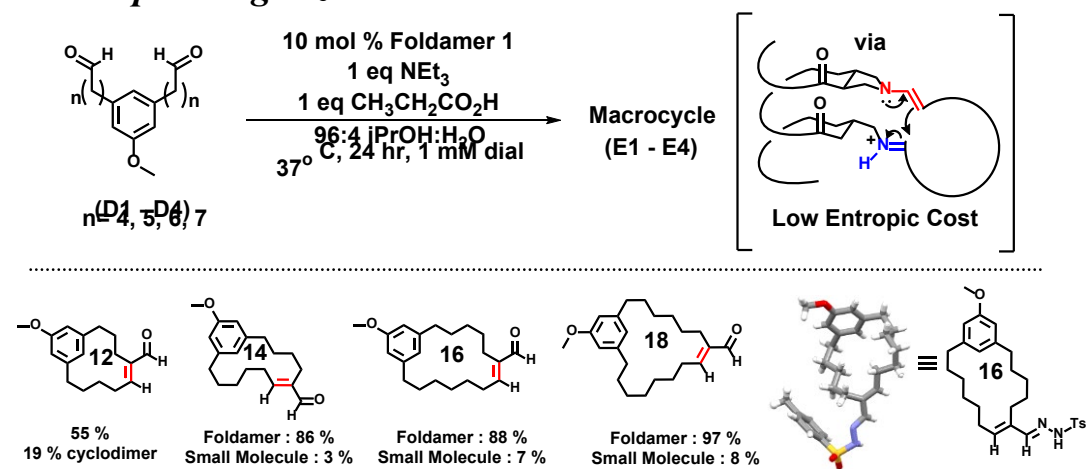


Fig. 1. Macrocyclization Strategies. (A) Prior approaches and foldamer approach to macrocyclization. (B) Divergent reactivity: foldamer vs. small molecule catalysis.

A Scope: Ring Size



B Structure-reactivity Relationship

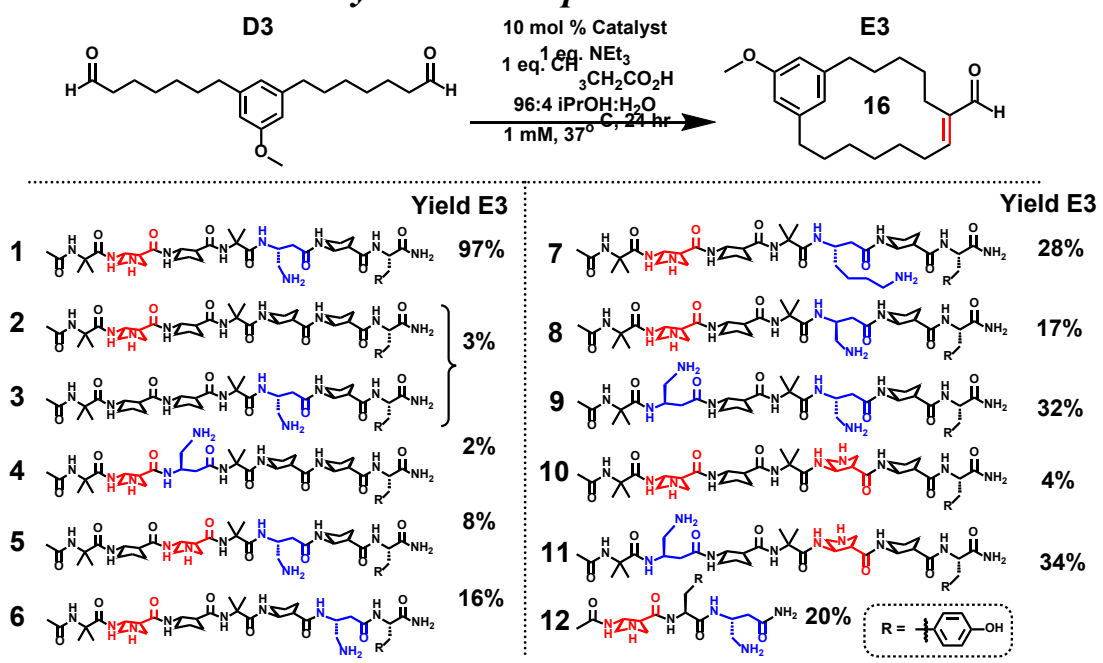


Fig. 2. Scope and structure-reactivity relationship. (A) Foldamer-catalyzed macrocyclization: ring size variation. Isolated yields are reported for foldamer-catalyzed reactions; however, yields for the pyrrolidine/n-butylamine catalyst pair (“small molecule”) are estimated based on LC-MS data. Ts = p-toluenesulfonyl. (B) Identification of features critical for foldamer catalysis of macrocyclization. Details are included in supplementary material (fig. S8-S12).

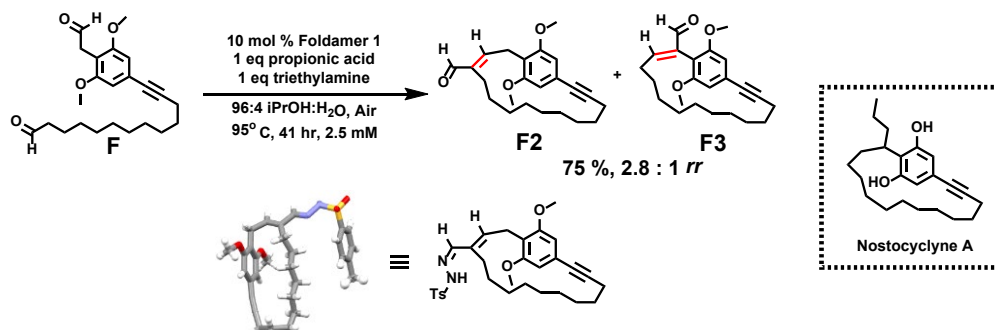
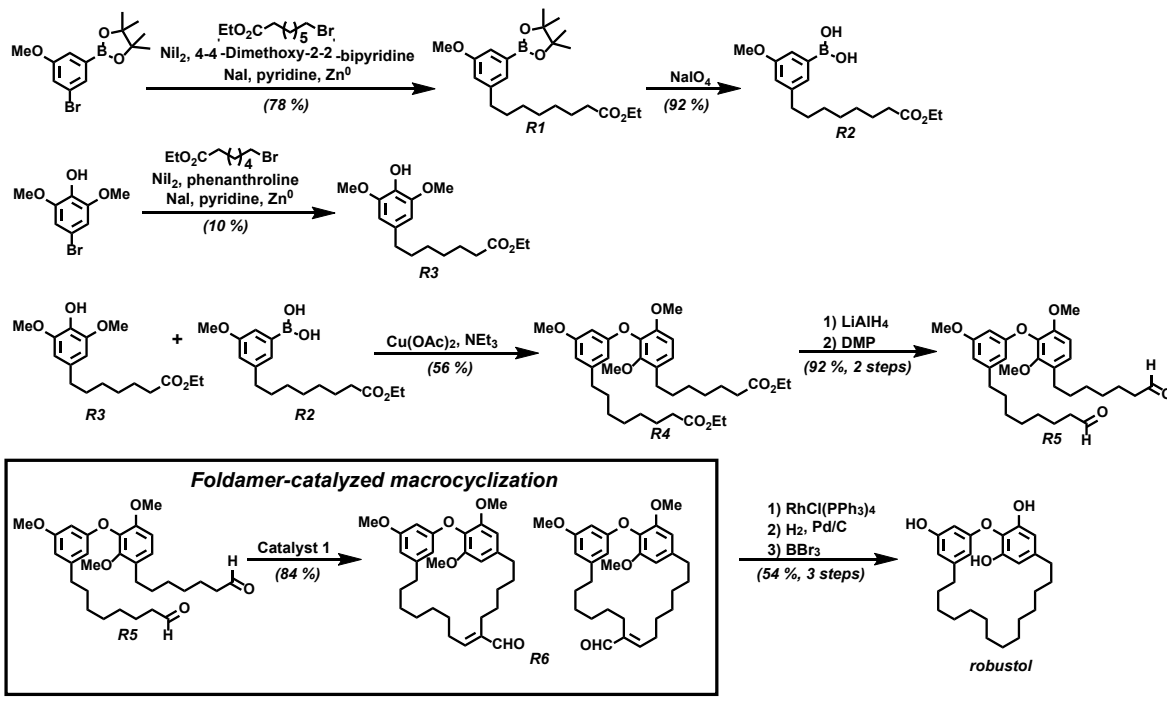
A**Macrocyclic Core of Nostocycline A****B****Total Synthesis of Robustol**

Fig. 3. Applications of foldamer catalysis in total synthesis. (A) Foldamer-catalyzed formation of the macrocyclic core of nostocycline A. Identity of product **F2** was established via the crystal structure of the tosylhydrazone derivative (Ts = p-toluenesulfonyl). **(B)** Total synthesis of robustol. The key step, foldamer-catalyzed closure of the 22-membered ring, is highlighted. See supplementary materials for full reaction protocols and product characterization.